Screening-photovoltaic bright solitons in lithium niobate and associated single-mode waveguides

E. Fazio,[a] F. Renzi, R. Rinaldi, and M. Bertolotti
Energetics Department, Università La Sapienza e INFM, Via Scarpa 16, I-00161 Roma, Italy

M. Chauvet
Laboratoire d'optique P.M. Duffieux, Universitè de Franche Comte, Besançon, France

W. Ramadan
Faculty of Sciences, University of Mansoura, Damietta, Egypt

A. Petris and V. I. Vlad
Romanian Center of Excellence in Photonics, Institute of Atomic Physics, NILPRP Bucharest, Romania

(Received 1 March 2004; accepted 28 July 2004)

Photorefractive screening-photovoltaic solitons are observed in lithium niobate. Two-dimensional bright circular solitons are formed thanks to a strong static bias field, externally applied, opposite to the photovoltaic internal field. The dynamics of the soliton formation is monitored and compared to a time-dependent numerical model allowing determination of the photovoltaic field. Efficient single mode waveguides are shown to be memorized by the soliton beam for a long time. © *2004 American Institute of Physics*. [DOI: 10.1063/1.1794854]

Lithium niobate ($LiNbO_3$) is a widely used material for optoelectronic applications due to the numerous properties (electro-optic, photovoltaic, pyroelectric, piezoelectric) it offers. $LiNbO_3$ also displays strong photorefractive properties useful for applications such as volume holographic storage[1] or spectral filters.[2] Planar and channel waveguides in $LiNbO_3$ can be produced either by proton exchange or by direct UV writing[3] or, as decently demonstrated, by dark solitons, that leave the material modified for a long time.[4] This last procedure is really attractive because soliton waveguides are by definition single mode structures.[5] Dark photovoltaic (PV) solitons have been observed in $LiNbO_3$,[6,7] due to the defocusing nature of the photovoltaic effect, even if bright screening-PV solitons[8] have been assumed by the application of static biases stronger than the photovoltaic field. Bright solitons are much more stable than dark solitons and offer the simplest way to photo-induce slab and channel waveguides. The application of intense biases has been already tested[9,10] with other photorefractive materials, and in this letter will be applied to induce bright solitons in congruent undoped $LiNbO_3$.

The scheme of the experimental setup is shown in Fig. 1. A congruent $LiNbO_3$ crystal is electrically biased along its optical z-axis (c-axis) direction. A laser beam at 514 nm, polarized along the z axis, is focused down to about 10 μm on the input face (Fig. 2) of the crystal and propagated along the 5-mm-long x axis (five diffraction lengths). A background beam at the same wavelength, mutually incoherent to the first one, is sent along the y axis. The beam shape evolution at the output planes is shown in Fig. 2, for a static bias field of 35 kV/cm, a background beam intensity of 1mW/cm^2, and a soliton peak intensity 1500 times more intense than the background intensity. Before the photorefractive effect takes place (0.0 min) the beam linearly diffracts. The self-focusing effect first starts along the optical z axis (direction of the applied field) and later on along the y direction. The confinement along the optical axis direction is almost complete after 10 min, while along the other direction the beam still evolves. After 17 min a minimum beam diameter is reached giving a soliton beam with a round shape. The initial Gaussian beam reshapes to a squared hyperbolic secant profile (see Fig. 3), confirming the soliton formation.[11] The normalized width of the soliton as a function of time is reported in Figs. 4(a) and 4(b). The fast axis [Fig. 4(a)], along the optical axis direction, and the slow axis [Fig. 4(b)] components of the profile have been fitted by exponential functions, whose time constants are, respectively, 3.3 and 5.5 min. A numerical calculation of the soliton formation was also performed using a one-dimensional beam propagation method where the time-dependent nonlinear photorefractive index change Δn as a function of the beam intensity distribution I is deduced from Ref. 12 with the addition of a background intensity I_b:

$$\Delta n = -\frac{1}{2} n_0^3 r_{33} \left(\frac{(E_0 + E_{\text{ph}})I}{I_n} + \frac{1}{I_n}\left(\frac{k_B T}{e} \frac{\partial I}{\partial x} \right) \right) \times \exp\left(-\frac{I_n}{I_d T_d} t \right) + E_0 \frac{I_b + I_d}{I_n} - E_{\text{ph}} \frac{I}{I_n} - \frac{1}{I_n}\left(\frac{k_B T}{e} \frac{\partial I}{\partial x} \right), \tag{1}$$

where n_0 is the extraordinary refractive index, r_{33} the electro-

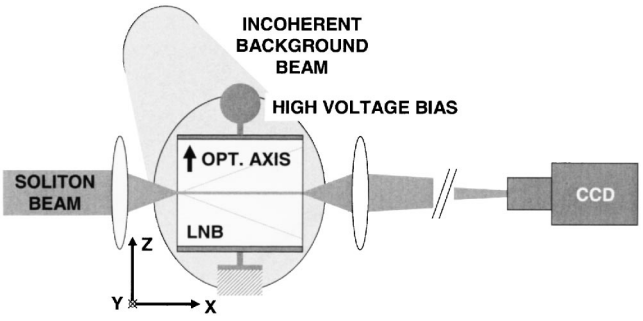

FIG. 1. Experimental setup.

[a]Electronic mail: eugenio.fazio@uniromal.it

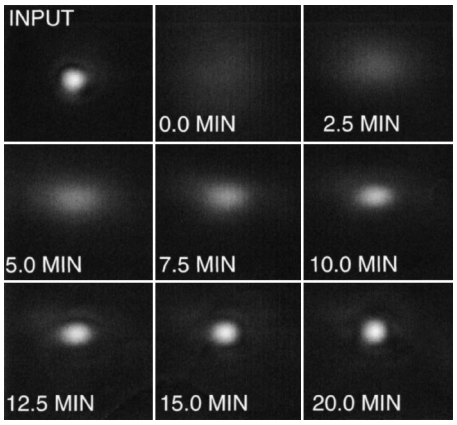

FIG. 2. Input and output beam waists after a dc bias of 35 kV/cm is turned on.

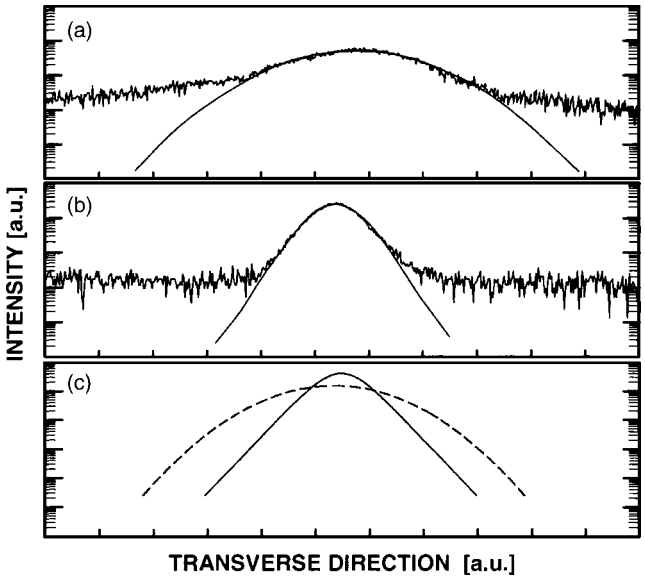

FIG. 3. The Gaussian beam profile 4(a) (a parabola in log scale) changes into a squared-hyperbolic secant when the soliton is formatted 4(b) (a cusp curve, as introduced in Ref. 12). This behavior has been confirmed numerically 4(c) for both Gaussian (dotted line) and soliton regimes (continuous line).

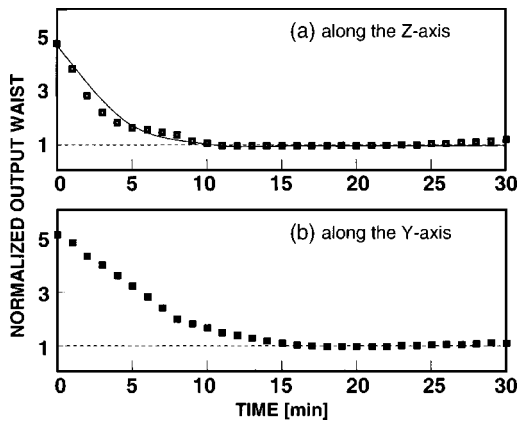

FIG. 4. Experimental waist dimension with numerical fit from the theoretical model for 35 kV/cm of bias: (a) along the *z* axis; (b) along the *y* axis.

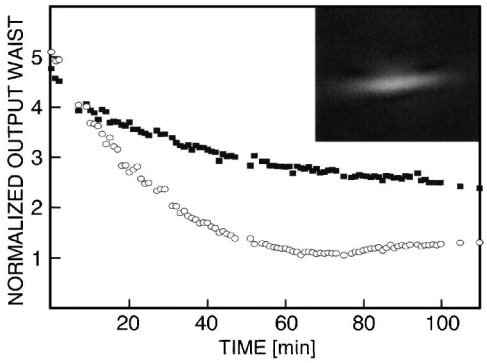

FIG. 5. As in Fig. 4 for 20 kV/cm of bias. Open circles: *z* axis; closed squares: *y* axis. The beam is not completely confined even after 1 h, as shown in the small image at the right top corner.

optic coefficient, E_0 the applied field, E_{ph} the photovoltaic field, k_B the Bolzmann constant, T the crystal temperature, e the electron charge, T_d the dielectric response time of the medium in the dark, I_d the equivalent dark irradiance, and $I_n = I + I_b + I_d$. Using the experimental parameters and $I_d \ll I_b = 1\text{mW cm}^{-2}$, $I_{max}/I_b = 1500$, $r_{33} = 32$ pm/V, $n_0 = 2.2$, $k_B T/e = 25$ mV, the theoretical beam profile evolution as a function of time has been computed [Fig. 4(a): fitting line]. E_{ph} was used as a free parameter and was set to -24.5 kV/cm for optimum beam width fitting while the free parameter $I_d\, T_d$ was set to 750 W cm^{-2} s for the best temporal fitting. These two parameters are characteristics of the $LiNbO_3$ crystal used. The calculated soliton propagation corresponding to the experiment shows that the initial Gaussian beam, the dotted line in Fig. 3(c), reshapes in less than 1 mm to a hyperbolic secant profile, the continuous line. This confirms the experimental behavior previously reported [see Figs. 3(a) and 3(b)]. Experimentally soliton bending due to charges diffusion[13] is also visible, as large as $\approx 10\ \mu$m, a bit larger than the theoretically predicted value (2.5 μm).

Applying lower voltages for bias, the kinetic of the soliton formation is much lower: for example at 20 kV/cm (see Fig. 5) the beam gets a solitonic shape along the bias direction (open circles in the figure) after almost 1 h, while the other direction (closed squares) is slightly focusing.

The solitonic path, after the light is switched off, remains written for long time, and can be used as a single-mode waveguide even months after its formation. In Fig. 6 we

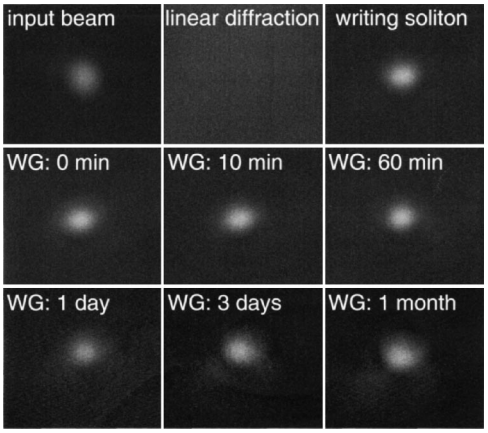

FIG. 6. Waveguiding properties of the solitonic channels. The images show both the soliton writing process and the waveguide modal profile as a function of the age time.

have reported the soliton writing the waveguide, as well as the modal profile of the solitonic waveguide up to 1 month from its formation. No effective degradation of the mode profile, and consequently of the waveguide, has been observed so far.

In conclusion this letter shows the formation of screening-photovoltaic solitons. Two-dimensional bright solitons have been obtained in congruent $LiNbO_3$ samples. The dynamic of the soliton formation is depicted and the guiding properties of the photo-induced waveguides have been evaluated. The results are modeled with a numerical model that allows evaluation of the photovoltaic field.

This work has been partially supported by Project No. 36 of the Bilateral Collaboration Agreement in R&D between Italy and Romania "AMDG."

[1]G. W. Burr, C. M. Jefferson, H. Coufal, M. Jurich, J A. Hoffnagle, R. M. Macfarlane, and R. M. Shelby, Opt. Lett. **26**, 444 (2001).
[2]J. Hukriede, D. Runde, and D. Kip, J. Phys. D **36**, R1 (2003).
[3]S. Mailis, C. Riziotis, I. T. Wellington, P. G. R. Smith, C. B. E. Gawith, and R. W. Eason, Opt. Lett. **28**, 1433 (2003).
[4]G. Couton, H. Maillotte, R. Giust, and M. Chauvet. Electron. Lett. **39**, 286 (2003).
[5]M. F. Shih, Z. Chen, M. Mitchell, M. Segev, H. Lee, R. S. Feigelson, and J. P. Wilde, J. Opt. Soc. Am. B **11**, 3091 (1997).
[6]M. Taya, M. C. Bashaw, M. M. Fejer, M. Segev, and G. C. Valley, Phys. Rev. A **52**, 3095 (1995).
[7]Z. Chen, M. Segev, D. W. Wilson, R. Muller, and P. D. Maker, Phys. Rev. Lett. **78**, 2948 (1997).
[8]L. Jinsong and L. Keqing, J. Opt. Soc. Am. B **16**, 550 (1999).
[9]E Fazio, F Mariani, M Bertolotti, V Babin, and V Vlad, J. Opt. A, Pure Appl. Opt. **3**, 466 (2001).
[10]E. Fazio, W. Ramadan, A. Belardini, A. Bosco, M. Bertolotti A. Petris, and V. I. Vlad, Phys. Rev. E **67**, 026611 (2003).
[11]E. Fazio, M. Zitelli, M. Bertolotti, A. Carrera, G. Chiaretti, and N. G. Sanvito, Opt. Commun. **185**, 331 (2000).
[12]N. Fressengeas, J. Maufoy, and G. Kugel, Phys. Rev. E **54**, 6866 (1996).
[13]M. I. Carvalho, S. R. Singh, D. N. Christodoulides, Opt. Commun. **120**, 311 (1995).